Direct Wigner Tomography of a Superconducting Anharmonic Oscillator

Yoni Shalibo,[1] Roy Resh,[1] Ofer Fogel,[1] David Shwa,[1] Radoslaw Bialczak,[2] John M. Martinis,[2] and Nadav Katz[1]

[1]*Racah Institute of Physics, The Hebrew University of Jerusalem, Jerusalem 91904, Israel*

[2]*Department of Physics, University of California, Santa Barbara, California 93106, USA*

(Received 12 August 2012; revised manuscript received 6 January 2013; published 5 March 2013)

The analysis of wave-packet dynamics may be greatly simplified when viewed in phase space. While harmonic oscillators are often used as a convenient platform to study wave packets, arbitrary state preparation in these systems is more challenging. Here, we demonstrate a direct measurement of the Wigner distribution of complex photon states in an anharmonic oscillator—a superconducting phase circuit, biased in the small anharmonicity regime. We apply our method on nondispersive wave packets to explicitly show phase locking in states prepared by a frequency chirp. This method requires a simple calibration, and is easily applicable in our system out to the fifth level.

DOI: 10.1103/PhysRevLett.110.100404 PACS numbers: 03.65.Wj, 03.67.−a, 42.50.−p, 85.25.Cp

The state of open quantum systems is frequently represented by a density matrix [1,2]. This description is useful for a wide variety of systems, in which the probabilities and coherences in some chosen basis are of interest. In systems with continuous degrees of freedom, e.g., the relative position and momentum of atoms in a molecule, wave packets are often formed and therefore phase space distributions are better suited to characterize the state and its dynamics [3]. In particular, the Wigner distribution offers direct information about expectation values and purity, and provides a convenient framework to test the quantum-classical correspondence [4,5]. Since the Wigner distribution is a representation of the density matrix, it is useful for quantum state tomography [6] as well. Numerous experiments measured the Wigner distribution in harmonic systems [7–9]. However, while anharmonic systems exhibit a wider variety of phenomena, a full quantum state reconstruction has so far been limited to atomic and molecular systems [10–13].

In this Letter, we report on a direct measurement of the Wigner distribution in the Josephson phase circuit, a superconducting anharmonic oscillator. Our method utilizes simple tomography pulses, and as opposed to standard state tomography (SST) [6], does not require individual calibration of the pulses [14].

Measuring the Wigner distribution in an anharmonic system poses several challenges. First, the phase of each level ϕ_n in the rotating frame advances increasingly with n, causing wave packets to disperse during the tomography pulse. For example, in a cubic potential this rate is given by $\dot{\phi}_n \approx \beta n(n-1)/2$, where $\beta = 2\pi(f_{10} - f_{21})$ is the anharmonicity and $n = 0, 1, 2, \ldots$. Second, in our system it is impossible to measure the probability distribution in the phase space quadratures directly, and therefore the prominent method for phase-space tomography is measurement of the parity after a coherent displacement [8]. In order to achieve an approximate displacement operation, one has to apply a pulse which is simultaneously resonant with all the transitions within the measured subspace. We find that both restrictions can be practically met by both reducing the anharmonicity and applying sufficiently short tomography pulses.

Our system, the Josephson phase circuit [16], is a superconducting LC oscillator with a weak anharmonicity, originating from a Josephson junction [17]. The potential energy of the system is one dimensional and has the form of a double well as a function of the phase difference δ across the junction. Using an external bias current I_b we tune the anharmonicity and measure the occupation probabilities of the energy levels inside the smaller potential well [see Fig. 1(b)]. The levels are excited using resonant microwave pulses $I_{\mu w}$, which can be simultaneously coupled to many levels at small anharmonicity ($\beta/2\pi f_{01} \sim 0.002$) [16]. The state is readout in the energy basis by applying a short pulse in I_b that causes level-selective tunneling. Tunneling events are measured via an on-chip SQUID [16].

In order to test this Wigner tomography scheme, we would like to create arbitrary multilevel states as inputs. This is difficult at small anharmonicity with short preparation pulses since the drive is simultaneously coupled to many levels and therefore the dynamics become complex. For longer pulses decoherence limits the state's purity, especially for multilevel states (for our system, the qubit decoherence parameters are $T_1 = 120$ ns and $T_2 > 150$ ns). We solve this difficulty, creating arbitrary, complex photon states, using a genetic optimization protocol. We apply this optimization directly in the experiment, without any assumption on the system's parameters, which is more robust to calibration errors. During an optimization we mutate and selectively breed pulse sequences (genomes) such as to maximize the population overlap $\chi = \sqrt{\vec{P}_i} \cdot \sqrt{\vec{P}_m}$, based on the measured level populations $\vec{P}_m$ and the desired ones $\vec{P}_i$ [15]. Each genome is defined by a set of amplitudes and phases of the microwave excitation,

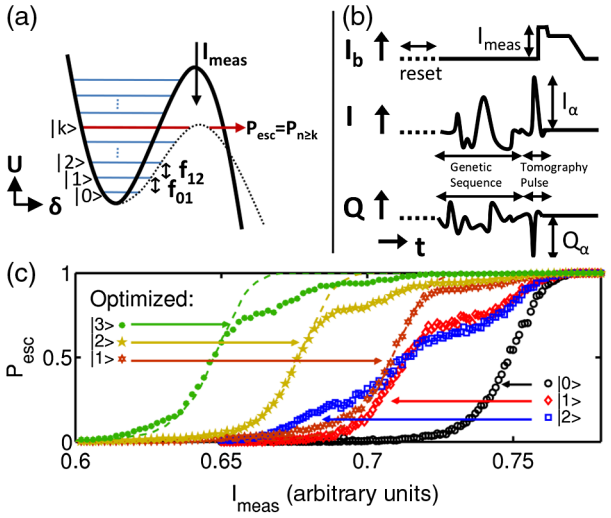

FIG. 1 (color online). Experimental techniques. (a) Measurement of the occupation probabilities using short pulses in bias I_{meas} that cause selective tunneling of states $n < k$ which are detected later with an on-chip SQUID. (b) Time sequence of the Wigner tomography measurement of Fock-type superpositions. (c) Tunneling measurements of optimized versus nonoptimized states at small anharmonicity as a function of measurement pulse amplitude. For the optimized states we used pulse sequences of length 20, 20, and 12 ns for the first, second, and third excited levels, respectively.

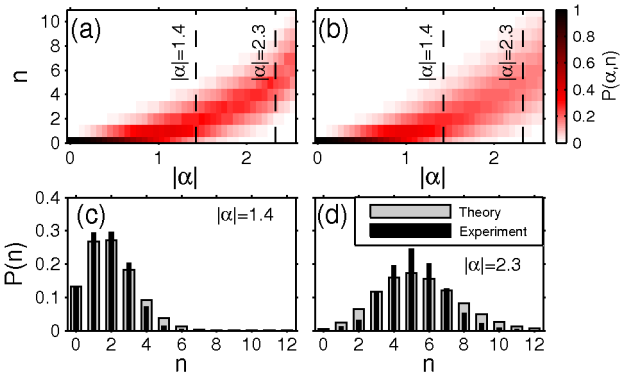

FIG. 2 (color online). Tomographic pulse. Occupation probabilities for levels $n \leq 12$, as a function of $|\alpha|$ in the experiment (a) and theory (b). (c), (d) Histograms along the dashed lines shown in (a) and (b).

set with a 1 ns time resolution. In Fig. 1(c) we measure the tunneling rates as a function of I_{meas} of optimized states at small anharmonicity. In this figure, we compare these measurements for states optimized manually to the 1st and 2nd excited levels (right) with ones optimized genetically (left) to the 1st, 2nd, and 3rd excited levels. The genetically optimized states are clearly much closer to the ideal dashed curves, as compared to the manually optimized states. We find that the population overlap increases sharply to more than 75% in less than ten iterations and then increases slowly as the algorithm progresses. As we show later, this technique is particularly useful for testing the Wigner tomography method.

Ideally, the Wigner distribution is proportional to the expectation value of the parity operator after a coherent displacement [18]. Because of the finite anharmonicity in our system, we use short, Gaussian-shaped resonant pulses as an approximate coherent displacement, while working at a weak anharmonicity. We control the phase and size of the complex displacement α by setting the phase and amplitude of the microwave pulse, using the relation $\alpha = -(1/2)\int \Omega(t)dt$ for a harmonic system, where $\Omega(t)$ is the time-dependent, Gaussian-shaped Rabi amplitude. For our experimental parameters [19], the pulse is simultaneously resonant with many transitions between consecutive levels, ~6 of which are subject to an amplitude variation of less than 10% from the peak amplitude [15]. For a given anharmonicity β, a resonant pulse can be well approximated by a harmonic displacement in the limit $\beta T|\alpha|m^2/4 \ll 1$, where $|\alpha|$ is the size of the applied displacement, m is the maximal occupied level after a displacement, and T is the pulse duration [15]. This condition limits the maximal displacement to be well below the size of the distribution in phase space ($|\alpha_{\max}| \ll 1$). However, we find in simulation that while the phases of the displaced state are sensitive to the above condition, the parity value remains insensitive for much larger displacements. We find that for our experiment parameters, up to 5 levels can be measured accurately. The expectation value of the parity operator is calculated from the measured occupation probabilities and is approximately given by $W(\alpha) = (2/\pi)\sum_n (-1)^n P_n$ for the lowest states in the well [15]. To test the effect of this pulse on our system, starting at the ground state we measure the occupation probabilities immediately after a short microwave pulse of total area α. Figure 2 shows the results of this measurement as a function of state number n and α [Fig. 2(a)], compared with the expected probabilities in a harmonic oscillator [Fig. 2(b)], $P(\alpha, n) = (1/n!)\exp(-|\alpha|^2)|\alpha|^{2n}$. As expected, the probability distribution in n is narrower compared to the harmonic system for higher amplitudes due to our finite bandwidth. To compare the data and theory quantitatively, we plot a histogram of the distribution [Figs. 2(c) and 2(d)] for $|\alpha| = 1.4$ and $|\alpha| = 2.3$. At $|\alpha| = 1.4$ our data fit well with a harmonic displacement. At the largest displacement values ($|\alpha| = 2.3$) the deviation from harmonicity becomes more apparent as expected [15], but is still small.

To benchmark our method, we apply it on a set of superpositions of eigenstates, $|\psi_l\rangle = (|0\rangle + e^{i\phi}|l\rangle)/\sqrt{2}$ [20]. These states have a simple structure in phase space and cannot disperse since they contain one measurable phase that results in only a free rotation. We use the genetic optimization to produce these states rapidly (~25 ns) at small anharmonicity (20 MHz). The results of the optimization algorithm are summarized in Table I. As expected, χ decreases for a larger n, mostly due to our relatively

TABLE I. Results of the optimization algorithm.

l	$P(\|0\rangle)$	$P(\|1\rangle)$	$P(\|2\rangle)$	$P(\|3\rangle)$	$P(\|4\rangle)$	$P(\|5\rangle)$	τ (ns)	χ (%)
1	0.52	0.47	0.01	0	0	0	15	99.8
2	0.69	0.05	0.24	0.02	0	0	30	93.4
3	0.58	0.03	0.11	0.27	0.01	0	25	90.5
4	0.70	0.01	0.03	0.07	0.17	0.02	40	88

short preparation pulse duration τ. To increase the value of χ for these states we increase τ, at the expense of the states' purity and optimization run time. Our optimization algorithm does not take into account phases; however, for sufficiently high values of χ, the Wigner image is dominated by only one phase, as can be seen in Fig. 3. In Fig. 3(a) we plot the results of the tomography measurement on the ground state, and states $|\psi_l\rangle$ described in Table I. In Fig. 3(b) we plot the density matrices of the measured states, extracted using the harmonic oscillator wave functions [15]. The diagonal elements in the extracted density matrices agree well with the measured occupation probabilities up to level $n = 4$. However, simulation shows that off-diagonal elements deviate increasingly for $n > 2$ [15]. We find that the origin of these errors is primarily the significant decay and decoherence that occur at highly excited levels during the tomography pulse. The errors in the measured Wigner distribution can be further reduced with currently available higher coherence samples [15]. States composed of more than 3 levels will tend to show an observable dispersion in the Wigner image, due to the accumulation of phases during the tomography pulse. However, these can be corrected using the time-reversed propagator of the bare system.

Wigner tomography of anharmonic oscillators is particularly useful to detect phase-locked states [21] since these are characterized by nondispersive dynamics in phase space. Phase locking to the drive may occur when the system is driven with a frequency chirp, such that the system's oscillation frequency follows that of the drive. This phenomenon occurs above an amplitude threshold, which depends on the chirp rate and anharmonicity. To measure this effect, we apply a negative frequency chirp ($\dot{f}_{\mathrm{drive}} < 0$), with a drive amplitude above the phase-locking threshold and a final frequency centered close to the transition frequency f_{23}. The chirp's temporal length and bandwidth $|f_{\mathrm{fin}} - f_{\mathrm{fin}}|$ are chosen to be short (20 ns) and large (600 MHz), respectively, in order to have a broad excitation of states and for the excitation to be adiabatic [16]. Figure 4 shows the result at selected times along the chirp [Fig. 4(a)], and after the drive is turned off [Fig. 4(b)]. The axes in the images are rotated at each time frame to fit the rotating frame of the drive. During the chirp, we see a displacement of the ground state distribution that gradually acquires a constant phase as the drive crosses the linear resonance ($f = f_{01}$). This happens, as expected, around $t = 16$ ns and the shape of the wave packet becomes crescentlike. After the drive is turned off ($t = 21$ ns), phase locking is lost and the wave packet disperses due to the finite anharmonicity. At $t = 35$ ns, the state has completely dispersed; however, it still contains significant coherences, as indicated by the negative values in the Wigner plot and the large off-diagonal elements in the extracted density matrix [Fig. 4(d)]. The state then dephases into a ring shape which shrinks in radius towards the ground state. To track decoherence dynamics in this experiment, we extract the state's purity evolution directly from the Wigner distribution: $\wp = \pi \int d\vec{\alpha} |W(\vec{\alpha})|^2$ [3]. The result is shown in Fig. 5 (red circles), and compared with a simulation (solid line). As expected, the purity remains high during the chirp, and then decays as a result of decoherence. The purity reaches a minimum and then ascends towards unity with an exponential rate, consistent

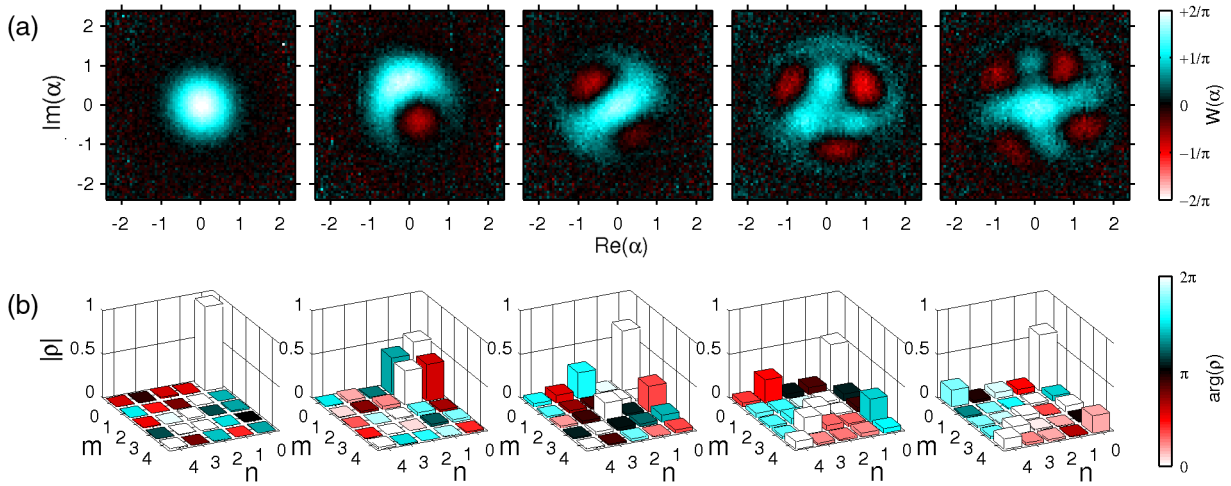

FIG. 3 (color online). Superposition of Fock-type states. (a) Wigner tomography of genetically optimized superposition of Fock-type states and (b) density matrices, extracted from the measurements shown in (a).

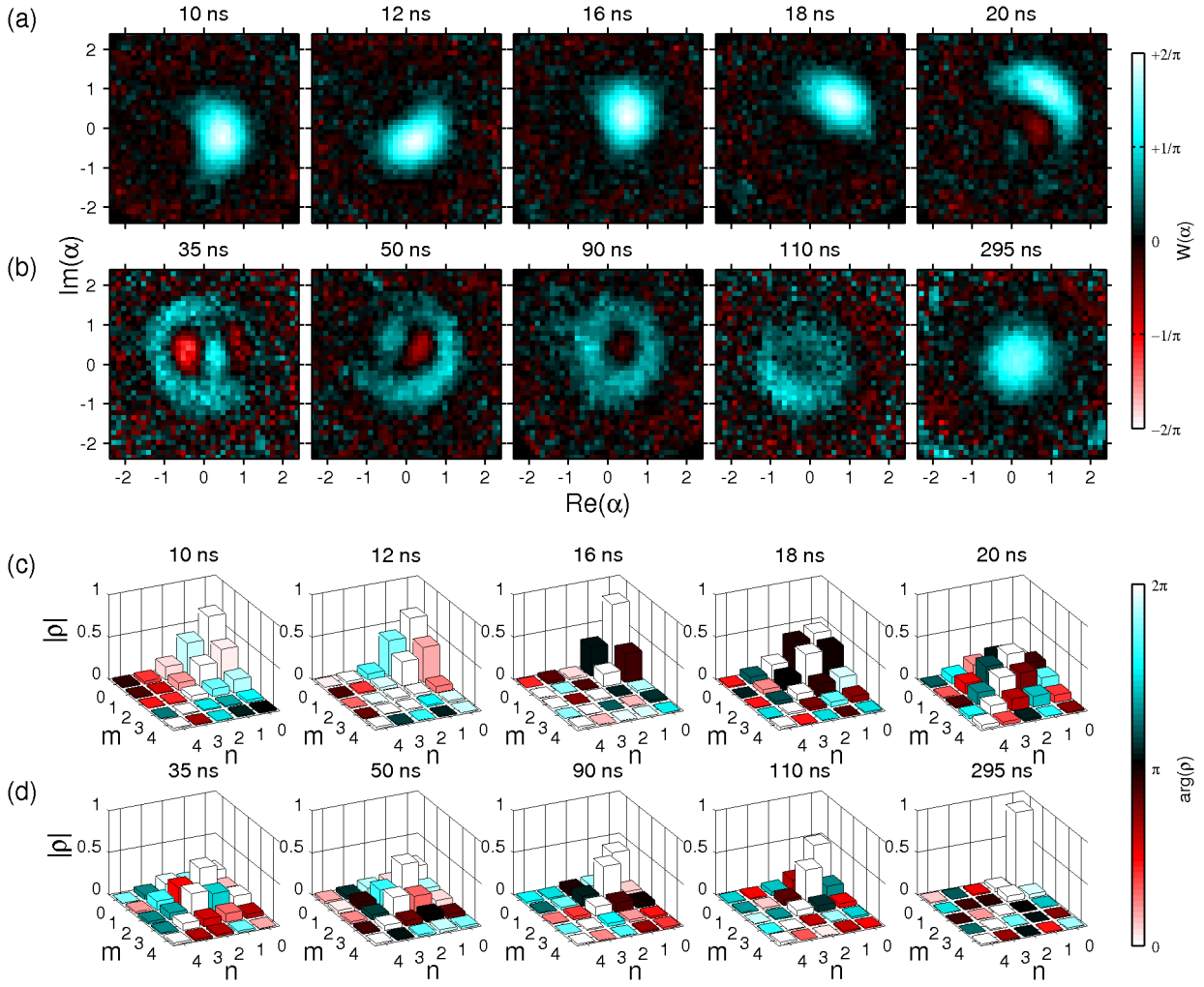

FIG. 4 (color online). Dynamics of a phase-locked wave packet. (a) Wigner tomography during a chirp ($T = 20$ ns, $\Omega/2\pi = 66$ MHz, $f_{\mathrm{in}} - f_{01} = 320$ MHz, $f_{\mathrm{fin}} - f_{01} = -50$ MHz) and (b) during drive-free evolution. (c), (d) Extracted density matrices for (a) and (b), respectively.

with the measured decay time ($T_1 = 120$ ns) and in accordance with simulation. This experiment opens the door for other measurements of wave packets in phase space. For example, it is possible to hold a phase-locked wave packet for long periods compared to T_1 [16] and generate cat states by multiple chirps.

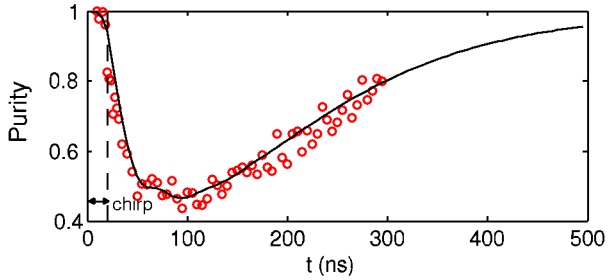

FIG. 5 (color online). State purity. Extracted state purity $\wp$ from experiments (red circles) and simulation (solid line) during chirp and decay. The simulation includes the effect of the decay and dephasing and agrees with the measured decay time.

In conclusion, we demonstrate a method of measuring the state of a multilevel system with a small anharmonicity in phase space. Using this method we are able to accurately extract the density matrix of up to 5 levels, limited by systematic errors caused by decoherence and finite bandwidth. This represents a significant improvement on SST which is difficult to implement in this subspace. The tunability of the phase circuit offers an approach of improving the accuracy of such a measurement at *larger* anharmonicity, by quickly changing the bias I_b after state preparation to the small anharmonicity regime where the tomography pulse is approximately a harmonic displacement.

We acknowledge fruitful discussions with David Tannor, Ronnie Kosloff, Omri Gat, and Ido barth. This work was supported by ISF Grant No. 1248/10 and BSF Grant No. 2008438.

[1] M. Steffen, M. Ansmann, R. C. Bialczak, N. Katz, E. Lucero, R. McDermott, M. Neeley, E. M. Weig, A. N. Cleland, and J. M. Martinis, Science **313**, 1423 (2006).
[2] L. DiCarlo, M. D. Reed, L. Sun, B. R. Johnson, J. M. Chow, J. M. Gambetta, L. Frunzio, S. M. Girvin, M. H. Devoret, and R. J. Schoelkopf, Nature (London) **467**, 574 (2010).
[3] W. P. Schleich, *Quantum Optics in Phase Space* (Wiley-VCH, Berlin, Germany, 2001), 1st ed.
[4] W. H. Zurek, Rev. Mod. Phys. **75**, 715 (2003).
[5] I. Katz, R. Lifshitz, A. Retzker, and R. Straub, New J. Phys. **10**, 125023 (2008).
[6] M. A. Nielsen and I. L. Chuang, *Quantum Computation and Quantum Information* (Cambridge University Press, Cambridge, England, 2004).
[7] P. Bertet, A. Auffeves, P. Maioli, S. Osnaghi, T. Meunier, M. Brune, J. Raimond, and S. Haroche, Phys. Rev. Lett. **89**, 200402 (2002).
[8] M. Hofheinz *et al.*, Nature (London) **459**, 546 (2009).
[9] C. Eichler, D. Bozyigit, C. Lang, L. Steffen, J. Fink, and A. Wallraff, Phys. Rev. Lett. **106**, 220503 (2011).
[10] T. J. Dunn, I. A. Walmsley, and S. Mukamel, Phys. Rev. Lett. **74**, 884 (1995).
[11] T. C. Weinacht, J. Ahn, and P. H. Bucksbaum, Phys. Rev. Lett. **80**, 5508 (1998).
[12] E. Skovsen, H. Stapelfeldt, S. Juhl, and K. Molmer, Phys. Rev. Lett. **91**, 090406 (2003).
[13] H. Hasegawa and Y. Ohshima, Phys. Rev. Lett. **101**, 053002 (2008).
[14] As we show in Ref. [15], there is a relatively small overhead in the number of tomography pulses required to extract the density matrix via Wigner tomography compared to SST.
[15] See Supplemental Material at http://link.aps.org/supplemental/10.1103/PhysRevLett.110.100404 for more details on the genetic algorithm and a numerical analysis of errors.
[16] Y. Shalibo, Y. Rofe, I. Barth, L. Friedland, R. Bialczack, J. M. Martinis, and N. Katz, Phys. Rev. Lett. **108**, 037701 (2012).
[17] J. Clarke and F. K. Wilhelm, Nature (London) **453**, 1031 (2008).
[18] A. Royer, Phys. Rev. A **15**, 449 (1977).
[19] We use a 1.6 ns FHWM pulse and an anharmonicity $\beta/2\pi = 20$ MHz.
[20] ϕ is an unknown phase that can be determined via Wigner tomography. Since our optimization algorithm is only sensitive to state populations and not to phases, we cannot know it in advance.
[21] J. Fajans and L. Friedland, Am. J. Phys. **69**, 1096 (2001).